Structure Of Flame Balls At Low Lewis-number (SOFBALL): Preliminary Results from the STS-83 Space Flight Experiments

Paul D. Ronney, Ming-Shin Wu and Howard G. Pearlman
Department of Aerospace and Mechanical Engineering
University of Southern California, Los Angeles, CA 90089

Karen J. Weiland
Microgravity Science Division
NASA Lewis Research Center, Cleveland, OH 44135

ABSTRACT

Results from the Structure Of Flame Balls At Low Lewis-number (SOFBALL) space flight experiment conducted on the STS-83/MSL-1 Space Shuttle mission are reported. These are the first premixed gas combustion experiments to be performed in space. Two of the fifteen scheduled tests were successfully completed on this shortened mission. Two different types of mixtures were burned, and both burned much longer than expected based on prior theoretical understanding. From these tests, two new insights were obtained, namely on the buoyancy-induced drift speed and repulsion of adjacent flame balls due to their mutual interaction. Preliminary results from the STS-94/MSL-1 reflight are also presented, which show a remarkable sensitivity of the flame balls to small accelerations resulting from Orbiter attitude control maneuvers. Comparison of experimental results to computational predictions reveals limitations in current models of H_2-O_2 chemistry for very lean mixtures. It is shown how the results of these space experiments may provide an improved understanding of the interactions of the two most important phenomena in combusting materials, namely chemical reaction and transport processes, in the unequivocally simplest possible configuration.

Corresponding author:

Prof. Paul D. Ronney
Department of Aerospace and Mechanical Engineering
University of Southern California
Los Angeles, CA 90089-1453
(213) 740-0490
(213) 740-8071 (fax)
ronney@usc.edu

Published in *AIAA Journal*, Vol. 36, pp. 1361-1368 (1998).

INTRODUCTION

Flames are typically classified as "premixed" flames, where all reactants (for example fuel and air) are intimately mixed on the molecular level before the combustion process is started, and "nonpremixed" or "diffusion" flames, where the fuel and oxidant must mix before combustion can take place. Premixed flames include the familiar laboratory Bunsen burner as well as the flame inside of a gasoline-fueled internal combustion engine. It is well known that premixed gas flames containing too little fuel ("lean mixtures") or too much fuel ("rich mixtures") will not burn. Despite many years of study, these lean and rich "flammability limits" and the behavior of weakly burning flames near these limits are not well understood. For example, the best available predictions of the burning velocities of very lean hydrogen-air mixtures near flammability limits are higher than the experimental measurements by a factor of 2[1]. Away from these limits, the agreement between model and experiment is much more satisfactory. Understanding combustion under lean conditions is critical to the design of efficient, clean-burning combustion engines. Lean-burning hydrogen-fueled engines are frequently considered as a means of meeting California's upcoming ultralow emission vehicle standards and the proposed federal emission standards for beyond the year 2000. Also, knowledge of near-limit behavior of flames is necessary for the assessment of fire and explosion hazards in mine shafts, oil refineries and chemical plants[2].

It has been known for many years[2] that most near-limit phenomena are influenced by gravity through the effects of buoyant convection on the transport rates of thermal energy and reactants to/from the chemical reaction zones. This has motivated a number of recent experiments on flame propagation in a μg environment[3,4]. It has been found that in a μg environment the absence of buoyant convection emphasizes other transport mechanisms, including the unequal rates of diffusion of thermal energy and diffusion of molecular reactants (the Lewis number effect) and the spectral radiation emitted from the gaseous combustion products. As a consequence of the change in the relative magnitudes of various transport mechanisms at μg, a number of new near-limit phenomena have been observed. Perhaps the most unusual of these are "flame balls," which are the subject of the SOFBALL flight experiment.

SCIENTIFIC BACKGROUND

Over 50 years ago, Zeldovich[5] showed that the steady heat and mass conservation equations admit a solution corresponding to a stationary spherical flame or "flame ball" (Fig. 1), just as the same governing equations in planar geometry admit a steadily propagating flame as a solution for every mixture. In the former case the solutions are characterized by a radius (r_*) and in

the latter case by the burning velocity. The mass conservation equation in a steady spherically symmetric system with no sources or sinks, $\nabla\cdot(\rho\mathbf{u}) = 0$, requires that $\mathbf{u}$ be identically zero everywhere. In spherical geometry, the solution to steady, convection free diffusion equations for temperature and chemical species, $\nabla^2 T = 0$ and $\nabla^2 Y$, are of the form $c_1 + c_2/r$, where c_1 and c_2 are constants. This form satisfies the requirement that T and Y be bounded as $r \rightarrow \infty$. For cylindrical and planar geometry the corresponding forms are $c_1 + c_2 \ln(r)$ and $c_1 + c_2 r$, respectively, which are obviously unbounded as $r \rightarrow \infty$. For this reason theory admits steady flame ball solutions, but not "flame cylinder" or "flame slab" solutions. Zeldovich showed that for an adiabatic flame ball, the energy and species conservation equations could be combined to infer the temperature at the surface of the flame ball (T_*):

$$T_* = T_\infty + \frac{T_{ad} - T_\infty}{Le} \qquad (1),$$

thus the temperature profile is given by $T(r) = T_\infty + (T_* - T_\infty) r_*/r$. Zeldovich also showed that flame ball solutions are unstable and thus probably would not be physically observable, just as planar flames are frequently subject to instabilities which prevent them from remaining planar.

Forty years later after Zeldovich, seemingly stable flame balls were accidentally discovered in drop-tower experiments[6] in lean hydrogen-air mixtures (Le ≈ 0.3) and subsequently observed in drop-tower and aircraft experiments[7] in H_2-O_2-CO_2 (Le ≈ 0.2), H_2-O_2-SF_6 (Le ≈ 0.06) and CH_4-O_2-SF_6 mixtures (Le ≈ 0.3). The μg environment of the drop tower was needed to obtain spherical symmetry and to avoid buoyancy-induced extinction of the flame balls. The following sequence of phenomena was observed as the mixtures were progressively weakened by addition of air, inert gas or chemical inhibitor. For mixtures sufficiently far from flammability limits, flame balls consistently split into more flame balls, resulting in an expanding spherical front composed of many individual cells, similar to the cellular fronts resulting from the diffusive-thermal instability widely observed at 1g in mixtures with low Le. For weaker mixtures closer to the flammability limits, stable flame balls were observed. For still weaker mixtures all flames extinguished. It was concluded that flame balls would probably occur in all combustible mixtures with low Le for mixtures close to the extinction limits, however, the short duration of drop tower experiments and the substantial fluctuations in the acceleration level in aircraft μg experiments precluded definite conclusions.

These results were found to be qualitatively the same over the range $0.06 < Le < 0.3$, with H_2 and CH_4 fuels, with or without added CF_3Br (a chemical inhibitor) and at pressures from 0.5 to 3 atm, indicating that variations in Lewis number over this range, chemical mechanisms, and radiation spectra do not *qualitatively* influence these phenomena.

As predicted by Eq. (1), because of the Lewis number effects, in mixtures with Le < 1 the flame ball temperature T_* can be much larger than the adiabatic homogeneous flame temperature T_{ad}. In the case of H_2-O_2-SF_6 mixtures (which have Le ≈ 0.06, the lowest of the mixtures tested to date), values of T_{ad} as low as 465K have been found to exhibit flame balls. This temperature is far below the H_2-O_2 explosion limit temperature, thus such mixtures could not possibly exhibit plane flames.

The apparent discovery of stable flame balls motivated a search for a stabilizing mechanism. Zeldovich[5] had noted the possibility of heat losses stabilizing flame balls. The effects of volumetric radiative losses (*e.g.*, due to gas radiation) on flame balls were analyzed by Buckmaster and collaborators[8,9]. When the heat losses are not too strong, two stationary flame ball radii are predicted (Fig. 2), a "large" flame ball that is strongly affected by heat loss and a "small" flame ball that is nearly adiabatic, and when the losses are sufficiently strong no solutions exist, indicating a flammability limit. As the limit is approached, the difference between the radii of the "large" and "small" balls decreases to zero. Stability analyses[8,9] showed that all small flame balls are unstable to radial disturbances, *i.e.*, the flame will either grow outward from the equilibrium radius (and possibly develop into a propagating flame) or collapse inward and extinguish. The basic reason is that as the flame ball radius increases, the surface area to volume ratio decreases, thus the ratio of total heat release (which is proportional to the flame ball surface area) to total radiative heat loss (which is proportional to the flame ball volume) increases, thus the flame ball becomes weaker and shrinks. Conversely, if the radius decreases, the flame ball grows stronger and expands. Thus, flame balls with sufficient volumetric losses can be stable to radial disturbances. Large flame balls with weak heat loss effects, *i.e.*, far from the flammability limits, are predicted[8,9] unstable to three-dimensional disturbances, which is consistent with the observation of splitting cellular flames in these mixtures. Consequently, a portion of the large flame branch close to the extinction limits is stable to both types of disturbances, which is consistent with the experimental observations.

It has also been predicted[10] that stable flame balls can only exist for mixtures with mixtures having Le less than a critical value which is less than unity, which explains why flame balls are not observed for mixtures with Le less than but close to unity (e.g. CH_4-air) or larger than unity (e.g. C_3H_8-air), even for near-limit mixtures at μg. Instead, conventional propagating flames are observed under these conditions. The reason is that, according to Eq. (1), for Le > 1, $T_* < T_{ad}$, thus flame balls are weaker than plane flames and cannot benefit from curvature in the manner discussed above for Le < 1 mixtures.

Flame balls have several unique and interesting properties which indicate a number of practical applications. Since they are one-dimensional, steady and convection-free, they are the simplest possible type of premixed flame structure and therefore provide a useful test-bed for

theoretical and numerical models of the interaction between chemical and transport processes in flames, especially near flammability limits. Some of these interactions are not predicted well even by the best currently available models. For example, numerical simulations of flame ball properties[11,13] employing detailed chemical, radiation and transport models in a spherically symmetric system show that different published chemical reaction models for hydrogen-oxygen oxidation predict widely varying flame ball characteristics (Fig. 3), even though all of these models can accurately predict the burning velocities of flames in hydrogen-air mixtures farther away from the extinction limits (Fig. 4). This is particularly significant because models of hydrocarbon combustion chemistry must have an accurate H_2-O_2 sub-mechanism if they are to be able to model hydrocarbons accurately. Also, since flame balls can be observed in mixtures that are well outside the conventionally defined extinction limits, microgravity can be a more hazardous environment from the point of view of fire safety. Flame balls warrant particular concern because they do not propagate; this makes fire detection and suppression more difficult. This potential problem is compounded because hydrogen burns without visible radiation or smoke, and because sources of hydrogen abound on spacecraft (*e.g.*, in propulsion and fuel cell systems). Flame balls may also be relevant to the turbulent combustion of mixtures with low Lewis number because flame balls are more robust than plane flames (the computed[11] radiation-induced extinction limit of flame balls in lean H_2-air mixtures is 3.43% H_2, whereas for plane flames it is 11.1%.) Consequently, sufficiently strong turbulence may extinguish planar flames, whereas flame balls could persist under the same conditions. Hence, structures reminiscent of flame balls could be the prevalent ones in near-limit turbulent combustion of lean hydrogen-air mixtures in engines.

EXPERIMENTAL APPROACH

Based on the discussion above, the objectives of the SOFBALL experiment can be summarized as follows:

- Determine whether steady, stationary flame balls can exist in an extended-duration μg environment
- Assess the influence of gaseous radiation on flame ball size and stability
- Determine whether flame ball motion (if observed) is due to the non-zero gravity level (present to a small extent even in the Spacelab environment)
- Determine the effect of Lewis number and radiation on flame balls through the use of mixtures employing different diluent gases

The drop-tower and aircraft μg experiments suggest that a very long duration and high quality μg environment is necessary to assess the steady properties and stability limits of flame balls. A theoretical estimate of the time required can be made in the following way. The response time of flame balls is on the order of the time for thermal diffusion of energy from the near-field region of the flame ball to the far-field region. Theory[8,9] shows that the former region is characterized by radii of the order of r_* and the latter region is characterized by radii of the order of θr_*. Consequently, the far-field time scale is of the order $(\theta r_*)^2/\alpha$. Since typical values of r_*, θ and α are 5 mm, 10 and 20 mm^2/s, respectively, for lean H_2-air mixtures, a representative time scale for flame ball evolution is 125 s - much longer than the time available from drop-tower or aircraft facilities. This evolution time scale is confirmed by numerical simulations, as shown in Fig. 5. Another consideration is that the gravity level must be small enough that the flame balls are not significantly affected by convection. Since the drift velocity of flame balls based on aircraft μg data was found[7] to be $1.5(gr_*)^{1/2}$, and velocities on the order of α/r_* are sufficient to disturb flame balls[12], we require $g << 1.5 \times 10^{-4}\ g_o$. To insure that the conductive flux, represented by α/r_*, is significantly less than the convective flux, represented by the drift velocity, the acceleration level should be a factor of θ less than this, or $1.5 \times 10^{-5}\ g_o$. Another requirement is that the acceleration is small enough that the flame balls do not drift into the walls of the combustion chamber before at least one characteristic evolution time has elapsed. This coincidentally also requires a gravity level of $1.5 \times 10^{-5}\ g_o$ or lower in the combustion chamber employed, which has a radius of 160 mm. This required time and quality of μg indicate the need for space experiments. The SOFBALL experiment on MSL-1 provided the requisite μg environment. It should be noted, though, that these pre-mission estimates require some re-evaluation in light of the experimental results shown below concerning the flame ball drift velocities at very low g.

The SOFBALL experiments were performed in the Combustion Module-1 facility (Fig. 6), developed by the NASA-Lewis Research Center in Cleveland, Ohio. A cylindrical chamber of 320 mm inside diameter and 320 mm length was filled from one of 14 bottles containing a pre-specified weakly combustible gas mixture and ignited using electric sparks of variable deposited energy up to 700 mJ with spark gaps variable from 0.35 to 10 mm; energies of 700 mJ and gaps of 5 mm and 2 mm, respectively, were used for the H_2-O_2-CO_2 and H_2-air tests described below. The flame balls evolving from this ignition source were observed using two intensified video cameras (sensitive to visible and near-IR emissions from 400 to 900 nm) with orthogonal views, a set of six thermocouples to measure gas temperature, and four radiometers (two unfiltered and two with a 5μm - 7.5μm band-pass filter to detect only H_2O radiation) to measure the radiant heat flux emitted from the flames. Additionally, the chamber pressure was recorded during the test and the on-orbit

acceleration levels were measured by four different on-board accelerometer instruments. The CM-1 facility is also equipped with a gas chromatograph for measuring the concentrations of all major reactant and product species, however, because of the time required for warm-up, flushing and calibration, it was not possible to employ this instrument during the shortened mission.

EXPERIMENTAL RESULTS

Two of the fifteen scheduled SOFBALL experiments were successfully conducted during the shortened STS-83 mission on the evening of April 6, 1997. (One of the 14 bottles was filled to twice the pressure required for a single chamber fill, so that a test of the repeatability of the results could be performed; in this way a total of 15 tests were planned.) These two tests are described below, followed by interpretations of some of the phenomena observed therein.

Test #1: 4.9% H_2 - 9.8% O_2 - 85.3% CO_2.

Three flame balls formed within a few seconds after ignition. All three burned until the experiment timed out (as planned) 500 seconds later. The size of the flame balls was 2.5 mm to 4 mm, which is comparable to that observed in prior drop-tower and aircraft experiments. The flame balls appeared to be shrinking slightly and growing dimmer toward the end of the test, probably for the reasons discussed in the following section. A typical image of the observed flame balls is shown in Fig. 7. The flame balls drifted several tens of mm away from each other during the test, but the imaginary point at the "center of mass" of the three balls hardly moved at all during this 500 s period. Thus, the flame ball movement is likely due to an interaction of the balls rather than buoyancy-induced drift. Both of these mechanisms of flame ball drift are discussed in the following section. From one camera view such as that shown in Fig. 7, the true size of the flame balls cannot be determined. Further analysis of the video images will employ a 3-d stereo image velocimetry (SIV) data processing system with image distortion correction using synchronized data from both cameras, so that the true positions, sizes and drift velocities of the balls can be determined accurately for all tests.

The maximum temperature observed by any thermocouple was about 135˚C, which is far below any expected combustion temperature, indicating that no flame ball drifted close to any thermocouple junction for this test. The maximum radiometer reading occurred about 120 s after ignition and was about 0.7 W per ball. This peak was rather flat, staying within 30% of this value for about 350 s. Since an accurate determination of temperature profiles and radiant emissions requires knowledge of the precise position of the balls relative to the thermocouple junctions and radiometers, the SIV-generated position data will be used to infer these properties. The pressure

rise in the chamber (ΔP) peaked at 0.010 atm at about the same time as the radiometer readings peaked. Since the energy release associated with this pressure rise is $\Delta PV_1/(\gamma-1)$, $\gamma \approx 1.295$ for this mixture, it can be inferred that 214 J, or 0.6 W per ball over this 120 s period, was deposited in the gas. Therefore, the total heat release rate over this period was about 1.3 W per ball.

Flame ball sizes, temperature profiles and total heat release rates are examples of information that will be compared in detail to numerical models[11,13]. In the case of this H_2-O_2-CO_2 mixture, the numerical model predicts that no mixtures below 5.8% H_2 are flammable. Even for 5.8% H_2 and higher, the predicted flame ball radii are much smaller than those observed in drop tower and aircraft μg experiments. No similar large discrepancies are found for H_2-air mixtures such as that described in Test #2 below.

The discrepancies for H_2-O_2-CO_2 mixtures are believed to be due to the effect of reabsorption of emitted radiation by the CO_2 diluent gas, which is neglected in current models[11,13]. Reabsorption is expected to be important for the CO_2-diluted mixture because L for CO_2 at 1 atm and 300K is 42 mm, which is much smaller than the radius of the combustion chamber. (These effects are unimportant for H_2-air mixtures, where the only radiating specie is H_2O and L is on the order of 1 m for the flame ball conditions.) Consequently, for H_2-O_2-CO_2 mixtures much of the radiation emitted from within or near the flame ball will not be lost to the chamber walls but instead will be reabsorbed within the gas. An approximate theoretical model of flame balls including radiative reabsorption effects[14] predicts that as the absorption length scale decreases, the flame ball size increases and the flammability limit shifts to weaker mixtures, which is consistent with the observed discrepancies. A computational estimate of an upper bound for reabsorption effects in H_2-O_2-CO_2 mixtures was obtained[13] by artificially neglecting CO_2 radiation entirely in the numerical model, which is equivalent to assuming zero absorption length. Figure 8 shows that the actual flame ball radii are much closer to that predicted assuming this upper bound for reabsorption effects rather than that predicted without reabsorption. (Two definitions of calculated flame ball radii are shown in Fig. 8, the half-width of the intensity profile at one-third of the maximum intensity and the radius at the location of maximum heat release; only the former should be compared directly to the experimental results.) An addition to our existing numerical model of flame balls to include an accurate assessment of reabsorption effects using a detailed radiation model is being developed.

Test #2: 3.85% H_2 - 96.15% air

Four flame balls formed within a few seconds after ignition. A typical image of the observed flame balls is shown in Fig. 9. One ball hit a thermocouple wire about 30 s after ignition and split

into two balls. All five balls burned until 100 s after ignition, when one extinguished. Subsequently, other balls extinguished at 150, 190, 270, and 320 s after ignition. As with Test #1, the flame balls drifted several tens of mm away from each other during the test. The visible radius of the balls was 4.5 mm to 8 mm, which is comparable to but somewhat larger than that observed in prior drop-tower and aircraft experiments, and is much larger than the numerical prediction[13] of 2.6 mm for the visible radius defined in the same manner. It should be noted, however, that the predicted radius is very sensitive to the chemical model employed (Fig. 3).

For this test, unlike the previous one, all flame balls extinguished before the 500 s experiment time-out. This is probably because (1) there were more flame balls formed during this test, (2) each flame ball was larger than in the first test and (3) the fuel (hydrogen) diffusivity is higher in N_2 than in CO_2. All of these factors led to more volume of fuel being consumed per unit time in the second test. An estimate of the total burn time for various mixtures is given in the following section.

All balls shrunk as they evolved toward extinguishment. This is expected because theory predicts that for weaker mixtures, the flame ball size decreases (Figs. 3, 8 and 10). Consequently, as fuel is consumed the effective mixture felt by the flame ball becomes weaker and the flame ball becomes smaller. At some point the flammability limit is reached and the flame ball extinguishes. (The 500 s test duration was not sufficient for any of this to happen in Test #1.) Just before extinguishment, the flame ball radii were about 2 mm. This is close to the predicted flame ball radius at extinguishment (Fig. 10), which suggests that the flame balls are evolving in a quasi-steady manner. Unfortunately, since it was not possible to use the gas chromatograph on the shortened mission, we were unable to compare the measured composition at extinguishment to the theoretical predictions.

As mentioned above, for this test it was not expected that radiative reabsorption effects would be important because L is larger than the size of the combustion chamber for the H_2-air combustion products. Thus, better (though still not very satisfactory) agreement between the experiment and the numerical model assuming optically-thin radiation can be expected and was observed for the H_2-air mixture than for the H_2-O_2-CO_2 mixture.

The gas temperature data obtained from this test are shown in Fig. 11, and the chamber pressure and radiometer data are shown in Fig. 12. These data are much more dynamic than that from the previous test, which is expected since 5 balls of varying size were observed and all extinguished at varying times during the test. The maximum temperature observed was 576˚C, which compares to the maximum predicted[13] temperature of 862˚C. This discrepancy is not surprising considering that no flame ball was observed to make a “direct hit” on a thermocouple junction.

DISCUSSION

Buoyancy-induced flame ball drift

It had not been expected that the flame balls in Test #1 or Test #2 would last more than about half of the 500 s experiment time-out period because the drift velocity (v) of flame balls was expected to be given by the formula[7]

$$v \approx 1.5\sqrt{gr_*} \qquad (2).$$

This empirical relation was inferred from data on drift velocity obtained in KC-135 μg aircraft experiments, where accelerations are on the order of 10^{-2} g_o. According to Eq. (2), even at 1 μg, a flame ball with radius 3 mm will drift 129 mm, nearly the radius of the chamber, in 500 s. The form of Eq. (2), $v \sim \sqrt{gr_*}$, is that of a bubble rising in an inviscid fluid[15], which implies viscosity effects are negligible. This is reasonable for the conditions in the aircraft experiments, where 50 is a typical Reynolds number (Re) based on the observed g-induced drift velocity and the "equivalent buoyant radius" of the flame ball, inferred to be about five times the visible radius[7]. (The high-temperature, low density region of the flame ball extends far beyond the visible radius, as implied by Fig. 1, thus the volume of buoyant gas is much larger than the volume of the flame ball itself.) In contrast, at 1 μg, Re will be much less than unity and the viscous, creeping-flow relation for bubbles[15]

$$v = \frac{1}{3}\frac{gr_b^{\,2}}{\nu_o}\left(\frac{\rho_b}{\rho_o} - 1\right)\frac{\mu_o + \mu_b}{\mu_o + 1.5\mu_b} \qquad (3),$$

where the b subscript refers to the bubble properties, should be employed instead of Eq. (2). Modeling the flame ball as a bubble whose radius is the equivalent buoyant radius (= $5r_*$) mentioned above and using temperature-averaging of gas properties based on an approximate maximum temperature of 1200K, Eq. (3) becomes

$$v = 2.4\frac{gr_*^2}{\nu_o} \qquad (4).$$

A comparison of the integrated drift distances based on these two predictions, Eq. (2) and Eq. (4), is shown in Fig. 13. For these predictions, the measured acceleration levels are taken from the

low-frequency, high-resolution ASTRE sensor of the Microgravity Measurement Assembly (MMA) experiment on MSL-1. While the validity of Eq. (4) has not yet been confirmed, Fig. 13 suggests that the viscous effects may decrease the predicted drift rate considerably. This is an interesting example of circumstances where ground-based μg experiments led to inaccurate predictions of the behavior of a space experiment.

Maximum burn time

With the very low drift velocities observed on STS-83, it is possible that in many cases the flame balls could continue to burn until their fuel supply has been depleted sufficiently, as occurred in Test #2, rather than drifting into the chamber wall first. To determine how long the flame balls could burn, consider the following estimate. Neglecting the minor contribution of radiant heat loss from the interior of the flame ball, the temperature gradient at the surface of the ball is[8,9] $(T_*-T_o)/r_*$ and thus the total heat conducted away from the ball (and consequently the total heat release) is $4\pi k_*(T_*-T_o)r_*$. Therefore, fuel is consumed at a molar rate $4\pi nk_*(T_*-T_o)r_*/MQ$. The total moles of fuel in the chamber that can be consumed before extinction is $\Delta\chi_f PV_2/RT_o$. Finally, the time to extinction (t_{ext}) is estimated as the moles of fuel consumed before extinction divided by the molar consumption rate of fuel:

$$t_{ext} = \frac{\Delta\chi_f PV_2 MQ}{4\pi nk_* RT_o(T_* - T_o)r_*} \qquad (5).$$

With $\Delta\chi_f$ and r_* inferred from earlier ground-based μg experiments[7], t_{ext} is estimated as 1500 s for Test #1 and 580 s for Test #2, as compared to the experimental observations of >500 s and 320 s, respectively. The estimates are therefore high but of the right order of magnitude. As mentioned earlier, in Test #1, the flame balls appeared to be shrinking and growing dimmer toward the end of the test, which suggests that they would have extinguished at some time between 500 s and 1500 s. This overestimate of t_{ext} could have been expected because the estimate leading to Eq. (5) assumes that fuel is always distributed evenly throughout the chamber, whereas realistically fuel is depleted only from the region surrounding the flame balls, thus at extinction there will most likely be some regions that still contain a flammable mixture. It is also interesting to note that for one of the 3 atm H_2-O_2-SF_6 test points scheduled for the reflight of SOFBALL on STS-94, according to Eq. (5), if only one flame ball formed in this mixture it could burn for about 17 hours! Of course, g-induced drift could cause the flame ball to drift into the wall before this time, but over the course

of one complete orbit (1.5 hours), some of the accelerations would integrate out to zero, and thus the g-induced drift might a less significant factor in very long duration burns.

Flame ball mutual repulsion

It was found that in both tests the flame balls drifted apart from each other throughout the duration of the burn. This had been seen in drop tower tests, but the test durations had been too short to obtain meaningful data on separation rates. In the space experiments it was found that the drift rate continually decreased with time. Figure 14 shows the mean separation between the three flame balls seen in Fig. 7 as a function of time, and the mean radius of separation, determined by finding the radius of the circle passing through all three flame ball centers. The camera view (not shown) orthogonal to that seen in Fig. 7 shows three practically collinear balls, which indicates that in the view shown in Fig. 7, the plane of the flame balls is orthogonal to the axis of the camera lens, which in turn indicates that the measure of flame spacing seen in this view is a reasonably accurate indication of the true spacing.

A proposed mechanism of flame ball drift based on the mutual depletion of total enthalpy (chemical plus thermal) by two flame balls in the region between them is presented here. When two flame balls are in close proximity, they have two influences on each other: first, they deplete each other of reactants from the region between them (decreased chemical enthalpy) and two, they increase the temperature in the region between them (increased thermal enthalpy). Because of the enthalpy gradient, one side of the flame ball will have a temperature slightly greater than T_* while the other will be slightly lower, thus leading to differences in heat release rate on the two sides of the ball. It is proposed that the ball must drift in the direction of increasing total enthalpy at a rate whereby the convective transport of enthalpy to the ball balances this difference in heat release rate.

As mentioned in the Scientific Background section, the temperature and mass fraction profiles outside an *adiabatic* flame ball are given by[5,8,9]

$$T = T_o + (T_* - T_o)\frac{r_*}{r}; \quad Y = Y_o\left(1 - \frac{r_*}{r}\right) \qquad (5).$$

Thus, the total enthalpy (h) per unit mass = $QY + C_p(T-T_o)$ in the region outside the flame ball is not constant; its gradient is given by

$$\frac{dh}{dr} = C_p \frac{r_*}{r^2}(T_* - T_o)(Le - A) \qquad (6).$$

In Eq. (6), A is a parameter whose value is unity for an adiabatic flame ball and is zero if all of the thermal energy in the mixture has been removed via radiant heat loss. The latter is the relevant condition for flame balls having sufficient separation because at radii greater than about 20 flame radii, radiant heat loss reduces the gas temperature to essentially ambient[13], consequently A = 0 will be considered exclusively in the following analysis.

Now consider two flame balls separated by a distance S. Each flame ball will feel the enthalpy gradient caused by the other ball. This enthalpy gradient will cause a temperature gradient dT/dz along the flame surface of the flame ball of the order $(1/C_p)(dh/dr)$, where z is the coordinate along the line joining the two balls. Over a distance $2r_*$, the total temperature difference between the two sides of the ball is then $(2r_*)(r_*/S^2)(T_* - T_o)Le$.

To assess how this temperature difference affects the reaction rate on the surface of the ball, first note that the nominal heat release per unit surface area (q) of a flame ball is $k_*(T_* - T_o)/r_*$. For an Arrhenius reaction with temperature dependence proportional to exp(-E/RT), small temperature changes (small enough that the exponential can be linearized) will lead to a change in q between the two sides of the ball given by

$$q = \frac{k_*\left(T_* - T_o\right)}{r_*}\left(1 - \theta\frac{T(z) - T_*}{T_*}\right) \qquad (7).$$

For a temperature difference of $(2r_*^2/S^2)(T_* - T_o)Le$, the difference in heat release rate between the two sides of the flame ball Δq is

$$\Delta q = \frac{2\theta Ler_*k_*T_*}{S^2}\left(1 - \frac{T_o}{T_*}\right) \qquad (8).$$

Finally, if we assume that the flame ball migrates toward the fresh gas at a speed v in order to find fresh reactants at a rate which exactly compensates for the heat flux gradient, *i.e.*, $\Delta q = \rho_o v C_p(T_{ad} - T_o) = \rho_o v C_p(T_* - T_o)Le$, the drift velocity must be

$$v = \frac{2\theta\alpha_o r_*}{S^2}\frac{k_*}{k_o}\frac{T_* - T_o}{T_*} \qquad (9).$$

Eq. (9) indicates $v \sim 1/S^2$, and since $v = dS/dt$, this prediction can also be expressed as

$$S = \left[6 \frac{k_*}{k_o} \frac{T_* - T_o}{T_*} \theta \alpha_o r_* t \right]^{1/3} \qquad (10).$$

A more rigorous model[16] using activation energy asymptotics but based on the same physical principles yields

$$S = \left[\frac{9 \alpha_o r_* t}{1 - Le} \right]^{1/3} \qquad (11).$$

which has the same dependence on α_o, r_* and time. The predictions of Eq. (11) with the representative parameters for Test #1 ($T_* \approx 1200$K, $T_o = 300$K, $\alpha_o \approx 10$ mm^2/s, $r_* = 3$ mm, Le = 0.2) are shown in Fig. 14, where the formula has been multiplied to by $(8/\sqrt{3})^{1/3}$ to account for the additional gradient caused by presence of three rather than two flame balls as well as transformation of the prediction from mean spacing to mean radius of separation. The agreement between theory and experiment is fairly close, and so may indicate some validity for the proposed mechanism of flame ball drift.

RESULTS FROM STS-94

The entire MSL-1 payload was re-flown as STS-94 from July 1 to July 16, 1997. A complete discussion of the SOFBALL experiments on STS-94 is beyond the scope of this work, however, a very brief discussion is given here.

A total of seventeen test points were performed on STS-94, compared to the pre-mission plan of fifteen tests. All fifteen planned combustion tests (see Experimental Approach) plus two additional tests (obtained by creating gas mixtures from bottle residuals) were completed. Sixteen of these mixtures ignited. These mixtures produced from one to nine flame balls, with the mixtures having more fuel producing multiple flame balls. Most of the tests burned for 500 seconds, until the experiment timed out and a mixing fan extinguished the flames. (Unfortunately, it was not possible to change the experiment duration after the STS-83 mission but before the STS-94 mission, due to the time that would have been required to re-verify the control software.) Ten of these mixtures were ignited a second time (since there was ample remaining fuel in some cases) and eight of these burned for an additional 500 seconds.

The flame balls were found to be much more sensitive to Orbiter Vernier Reaction Control System (VRCS) thruster firings than expected pre-flight. These firings produced a noticeable change in the flame ball position, drift speed, and especially radiometer data (Fig. 15). The strong effect of microgravity disturbances on radiation is probably due to the fact that the visible flame ball is surrounded by a much larger volume of hot but non-reacting gas. Most of the radiation is emitted from this large gas volume rather than from within the flame ball itself[11]. This large ball of gas is extremely susceptible to buoyancy-induced motion resulting from even the smallest VRCS impulses (on the order of 50 μg for 1 sec = 0.5 mm/sec). (Careful inspection of the two data sets from STS-83 also showed this trend, but it was much less noticeable in these cases because both STS-83 tests produced multiple flame balls with more widely dispersed hot gas regions that, as a group, are much less affected by the VRCS firings than tests producing only one or two flame balls.) Note that Fig. 15 shows that only VRCS firings, which cause a net change in the Orbiter momentum, had any effect; vibrations resulting from crew and Orbiter systems operations, which do not affect the net momentum of the Orbiter, had practically no effect. Once the effects of the VRCS firings were seen, "free drift" (suppression of VRCS firings) was requested during the remaining experiments and was granted in many cases. When free drift could be maintained for the entire test period, the disturbances to the radiometer readings did not occur.

Preliminary inspection of the flight data suggest that the flame balls respond ballistically to the VRCS impulses, that is, the impulse (change in velocity) imparted to the ball is the same as the acceleration impulse. This change in velocity then decays on a time scale of tens to hundreds of seconds, which is comparable to the viscous time scale associated with the flame ball and its surrounding hot gas field.

SUMMARY AND CONCLUSIONS

Two space-based experiments on STS-83 have shown that flame balls are in fact stable for very long periods of time in a μg environment. This was the single most important science issue to be resolved, and for this reason the tests performed on the shortened mission can be considered successful. The rate at which the flame balls drift due to the small acceleration levels on the spacecraft was far smaller than that expected before the mission. A modified mechanism of buoyancy-induced drift is proposed based on the difference between the flow regimes in the aircraft and space experiments (nearly inviscid flow vs. creeping flow), and a new mechanism of flame ball drift induced by mutual interaction of adjacent flame balls is proposed.

It is clear based on these two space-based tests alone that at least two new modeling efforts will be required to obtain a detailed understanding of these results: (1) buoyancy-induced flame ball drift and (2) flame balls with reabsorption of emitted radiation (optically thick radiation).

Another finding of these experiments is that the differences between computer models and experiments found based on earlier short-duration μg tests were also found in the space experiments. Different models of H_2-O_2 chemistry yield different predictions for flame ball properties, and it is expected that detailed evaluation of the results of the space experiments will help lead to the identification of the most appropriate chemical models for lean-limit combustion of hydrogen and hydrocarbon fuels.

ACKNOWLEDGMENTS

A large number of individuals contribute to a successful space flight experiment; only a few can be named here. The authors wish to thank the CM-1 Project Managers, Mr. Roy Hager (retired) and Ms. Ann Over, the CM-1 Project Engineer, Mr. Ron Chucksa (retired) and the entire CM-1 engineering and operations team for their tremendous effort in designing, constructing, testing and operating the CM-1 facility. Scientific discussions with Prof. John Buckmaster and Dr. Guy Joulin have been invaluable. Angel Abbud-Madrid, Mohammed Abid, Quin Blackburn and Jian-Bang Liu assisted with the data analysis during and after the missions. Special thanks is owed Dr. Roger Crouch for performing the space experiments on STS-83, along with the rest of the STS-83 crew. This work was supported by NASA under grants NAG3-965, NAG3-1242 and NAG3-1523.

NOMENCLATURE

C_p	gas specific heat at constant pressure
D	mass diffusivity of stoichiometrically limiting reactant
E	activation energy
g	acceleration of gravity
g_o	earth gravity
h	enthalpy
k	thermal conductivity
L	Planck mean absorption length
Le	α/D (Lewis number)

M	fuel molecular weight
n	number of flame balls
P	pressure
Q	heating value of fuel per unit mass
r	radial coordinate
R	gas constant
Re	Reynolds number
S	separation distance between flame balls
T	temperature
T_{ad}	adiabatic flame temperature for homogeneous mixture
t	time
u	fluid velocity vector
v	drift velocity of flame ball (due to buoyancy or mutual repulsion)
V_1	total volume of combustion chamber (63 liters)
V_2	usable volume of combustion chamber (26 liters)
Y	mass fraction of scarce reactant

Greek characters

α	thermal diffusivity
γ	specific heat ratio
$\Delta\chi_f$	difference between initial fuel mole fraction and mole fraction at extinction
θ	E/RT_* (non-dimensional activation energy)
ν	kinematic viscosity
μ	dynamic viscosity
ρ	density

Subscripts

ext	extinction condition
o	ambient condition
*	at flame ball surface

REFERENCES

[1]Eolfopoulos, F. N. and Law, C. K., "An Experimental and Computational Study of the Burning Rates of Ultra-lean to Moderately-rich $H_2/O_2/N_2$ Laminar Flames with Pressure Variations," Twenty-Third Symposium (International) on Combustion, Combustion Institute, Pittsburgh, 1990, pp. 333-340.

[2]Coward, H. and Jones, C., "Flammability Limits of Gases and Vapors," U. S. Bureau of Mines Bulletin 503, 1952.

[3]Ronney, P. D., "Effect of Chemistry and Transport Properties on Near-Limit Flames at Microgravity," Combustion Science and Technology, Vol. 59, 1988, pp. 123-141.

[4]Abbud-Madrid, A. and Ronney, P. D., "Effects of Radiative and Diffusive Transport Processes on Premixed Flames Near Flammability Limits," Twenty-Third Symposium (International) on Combustion, Combustion Institute, Pittsburgh, 1990, pp. 423-431.

[5]Zeldovich, Ya. B., Theory of Combustion and Detonation of Gases, Academy of Sciences (USSR), Moscow, 1944.

[6]Ronney, P. D. "Near-Limit Flame Structures at Low Lewis Number," Combustion and Flame, Vol. 82, 1990, pp. 1-14.

[7]Ronney, P. D., Whaling, K. N., Abbud-Madrid, A., Gatto, J. L. and Pisowicz, V. L., "Stationary Premixed Flames in Spherical and Cylindrical Geometries," AIAA Journal., Vol. 32, 1994, pp. 569-577.

[8]Buckmaster, J. D., Joulin, G. and Ronney, P. D., "Effects of Heat Loss on the Structure and Stability of Flame Balls," Combustion and Flame, Vol. 79, 1990, pp. 381-392.

[9]Buckmaster, J. D., Joulin, G. and Ronney, P. D., "Structure and Stability of Non-adiabatic Flame Balls: II. Effects of far-field losses," Combustion and Flame, Vol. 84, 1991, pp. 411-422.

[10]Lee, C. and Buckmaster, J. D., "The Structure and Stability of Flame Balls: a Near-Equidiffusional Flame Analysis," SIAM Journal on Applied Mathematics, Vol. 51, 1991, pp. 1315-1326.

[11]Wu, M. S., Ronney, P. D., Colantonio, R. and VanZandt, D., "Detailed Numerical Simulation of Flame Ball Structure and Dynamics," to appear in Combustion and Flame (1998).

[12]Buckmaster, J. D. and Joulin, G., "Flame Balls Stabilized by Suspension in Fluid with a Steady Linear Ambient Velocity Distribution," Journal of Fluid Mechanics, Vol. 227, 1991, pp. 407-427.

[13]Wu, M. S. and Ronney, P. D., Twenty-Seventh Symposium (International) on Combustion, Combustion Institute, Pittsburgh, 1998, to appear.

[14]Lozinski, D., Buckmaster, J. D., Ronney, P. D., "Absolute Flammability Limits and Flame Balls in Optically Thick Mixtures," Combustion and Flame, Vol. 97, 1994, pp. 301-316.

[15]Batchelor, G. K., An Introduction to Fluid Dynamics, Cambridge University Press, Cambridge, U.K., 1967.

[16]Buckmaster, J. D. and Ronney, P. D., "Flame Ball Drift in the Presence of a Total Diffusive Heat Flux," Twenty-Seventh Symposium (International) on Combustion, Combustion Institute, Pittsburgh, 1998, to appear.

[17]Frenklach, M., *et al*., "An Optimized Kinetics Model for Natural Gas Combustion," Twenty-Fifth Symposium (International) on Combustion, Poster 26, Session 3, 1994.

[18]Peters, N. in: Reduced Kinetic Mechanisms for Applications in Combustion Systems, N. Peters and B. Rogg (Eds.), Springer-Verlag, Berlin-Heidelberg, 1993, Chapters 1 and 5.

[19]Yetter, R. A., Dryer, F. L. and Rabitz, H., "A Comprehensive Reaction Mechanism For Carbon Monoxide/Hydrogen/Oxygen Kinetics," Combustion Science and Technology, Vol. 79, 1991, pp. 97-128.

[20]Mauss, F., Peters, N., Rogg, B. and Williams, F. A., in: Reduced Kinetic Mechanisms for Applications in Combustion Systems, N. Peters and B. Rogg (Eds.), Springer-Verlag, Berlin-Heidelberg, 1993, Chapter 3.

FIGURE CAPTIONS

Figure 1. Schematic diagram of a flame ball, illustrated for the case of fuel-limited combustion at the reaction zone. The oxygen profile is similar to the fuel profile except its concentration is non-zero in the interior of the ball. The combustion product profile is identical to the temperature profile except for a scale factor.

Figure 2. Theoretical prediction[8] of the effect of heat loss on flame ball radius and stability properties with single-step Arrhenius chemistry, constant thermodynamic and transport properties and volumetric heat loss from the interior of the ball. The dimensionless radius is the ratio of r_* to the value of r_* for an adiabatic flame ball in the same mixture. The curve is valid for any Lewis number, but the stability properties shown apply to Le < 1 only.

Figure 3. Predicted[13] steady flame ball radii and radiant emission in H_2-air mixtures using the GRI[17], Peters[18] and Yetter[19] chemical models.

Figure 4. Predicted[13] steady burning velocities (S_L) of H_2-air mixtures using the GRI[17], Peters[18] and Yetter[19] chemical models. A compilation[20] of experimental results from several sources is also shown.

Figure 5. Predicted nonsteady evolution of a flame ball in a 4.02% H_2-air mixture[11]. "Radius" refers to radial location of maximum volumetric heat release rate; "heat release rate" and "radiative loss" refer to total values (integrated over all radii).

Figure 6. Schematic diagram of experimental apparatus test section.

Figure 7. Image of flame obtained in 4.9% H_2 / 9.8% O_2 / 85.3% CO_2 mixture, taken 130 s after ignition. Field of view is 112 mm x 150 mm.

Figure 8. Predicted[13] visible flame ball radii in H_2-O_2-CO_2 mixtures (H_2:O_2 = 1:2) (solid curve) along with measured flame ball radii from aircraft μg experiments[7] (squares) and preliminary measured radii for SOFBALL Test #1 (circles). Also shown are predicted[13] flame ball radii based on radial location of maximum heat release including and excluding CO_2 radiation (dashed curves). The GRI chemical mechanism[17] is used in the predictions shown.

Figure 9. Image of flame balls obtained in 3.85% H_2 / 96.15% air mixture, taken 25 s after ignition. Field of view is 112 mm x 150 mm.

Figure 10. Predicted[13] visible flame ball radii in H_2-air mixtures (solid curve) along with measured flame ball radii from aircraft μg experiments[7] (squares) and preliminary measured radii for Test #2 (circles). Also shown are predicted[13] flame ball radii based on radial location of maximum heat release (dashed curve). The GRI chemical mechanism[17] is used in the predictions shown.

Figure 11. Measured gas temperatures for Test #2. Thermocouple locations corresponding to GasTemp1 through GasTemp6 are 30, 50, 70, 90, 110 and 130 mm from spark gap, respectively.

Figure 12. Measured chamber pressure and radiant emissions for Test #2.

Figure 13. Flame ball drift distances predicted by the inviscid (Eq. (2)) and viscous (Eq. (4)) bubble rise relations for the conditions of Test #1, using acceleration data from the MMA/ASTRE system.

Figure 14. Observed radius of separation and mean separation of three flame balls in Test #1 as a function of time, and comparison to theoretical predictions[16].

Figure 15. Example correlation of radiometer readings with Orbiter acceleration environment during STS-94 mission showing impact of Vernier Reaction Control System (VRCS) thruster firings. Mixture: 6.50% H_2 - 13.00% O_2 - 80.50% SF_6, 1 atm initial pressure. This test produced 1 flame ball.

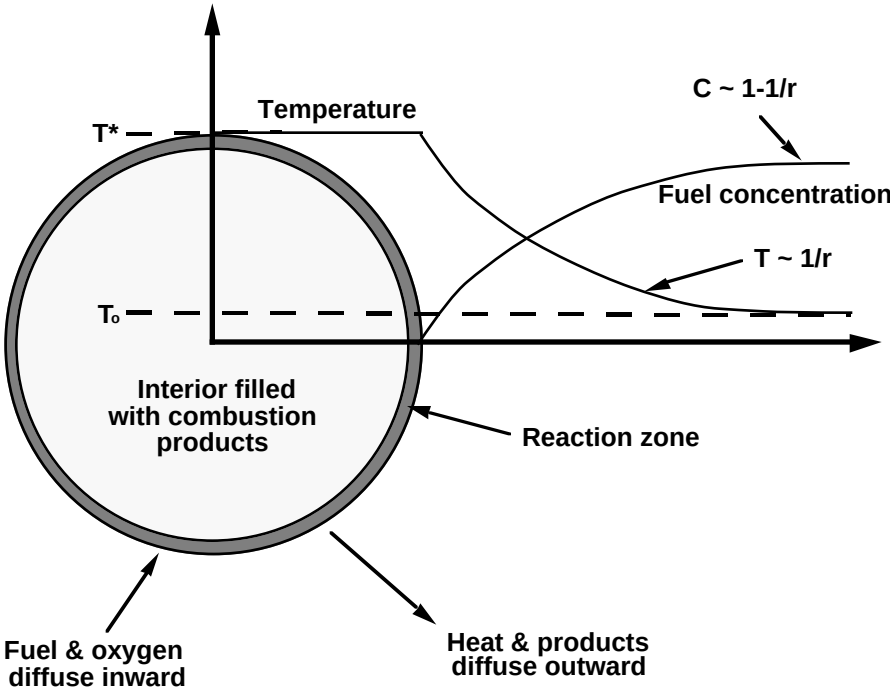

Figure 1. Schematic diagram of a flame ball, illustrated for the case of fuel-limited combustion at the reaction zone. The oxygen profile is similar to the fuel profile except its concentration is non-zero in the interior of the ball. The combustion product profile is identical to the temperature profile except for a scale factor.

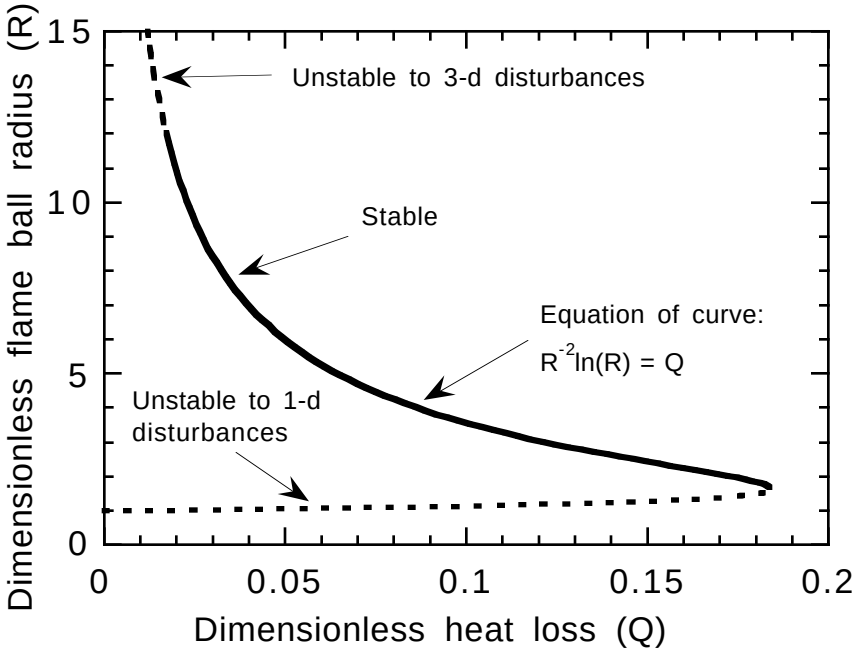

Figure 2. Theoretical prediction[8] of the effect of heat loss on flame ball radius and stability properties with single-step Arrhenius chemistry, constant thermodynamic and transport properties and volumetric heat loss from the interior of the ball. The dimensionless radius is the ratio of r_* to the value of r_* for an adiabatic flame ball in the same mixture. The curve is valid for any Lewis number, but the stability properties shown apply to Le < 1 only.

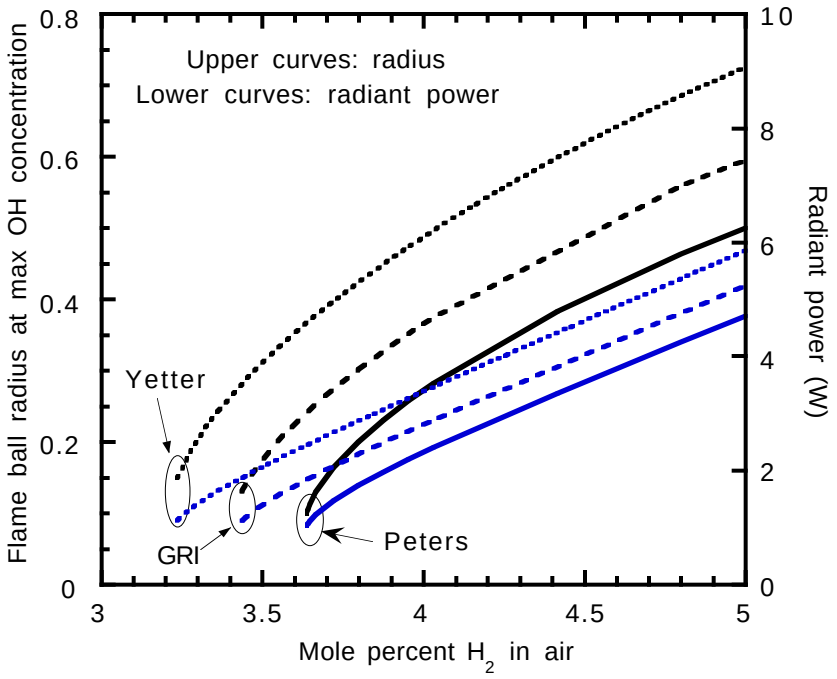

Figure 3. Predicted[13] steady flame ball radii and radiant emission in H_2-air mixtures using the GRI[17], Peters[18] and Yetter[19] chemical models.

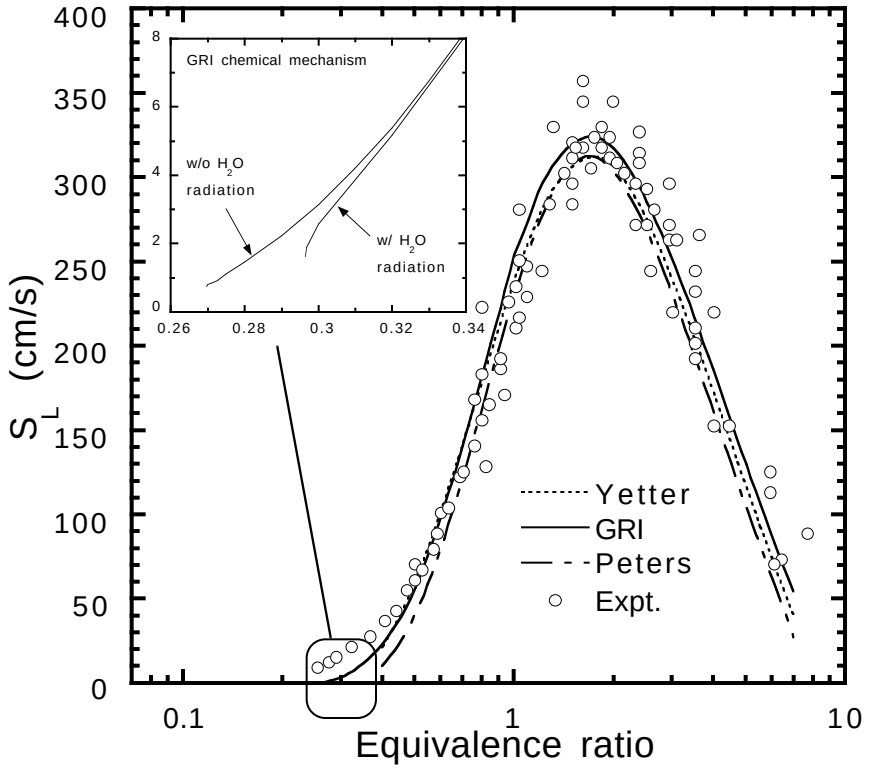

Figure 4. Predicted[13] steady burning velocities (S_L) of H_2-air mixtures using the GRI[17], Peters[18] and Yetter[19] chemical models. A compilation[20] of experimental results from several sources is also shown.

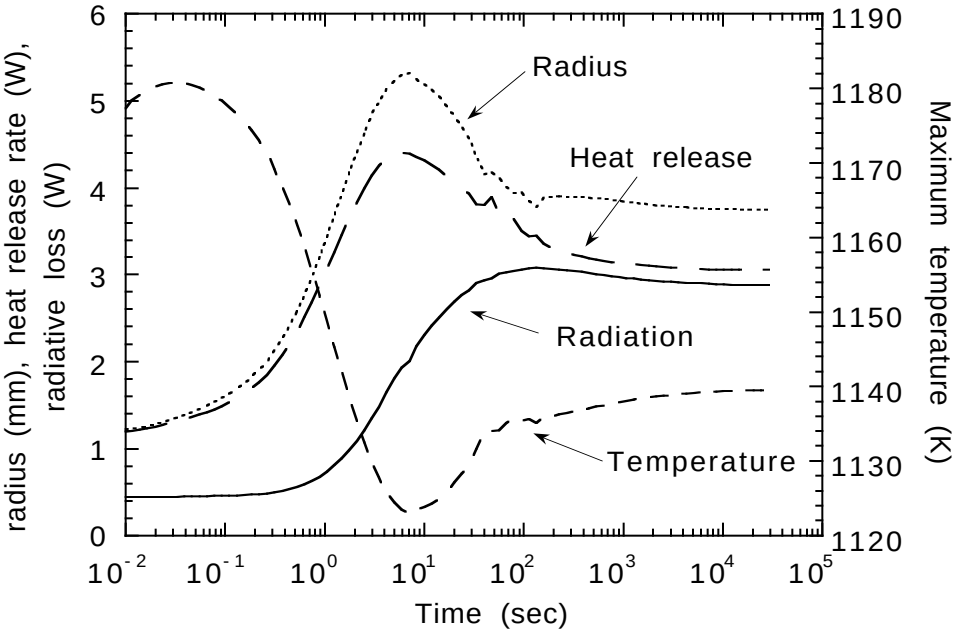

Figure 5. Predicted nonsteady evolution of a flame ball in a 4.02% H_2-air mixture[11]. "Radius" refers to radial location of maximum volumetric heat release rate; "heat release rate" and "radiative loss" refer to total values (integrated over all radii).

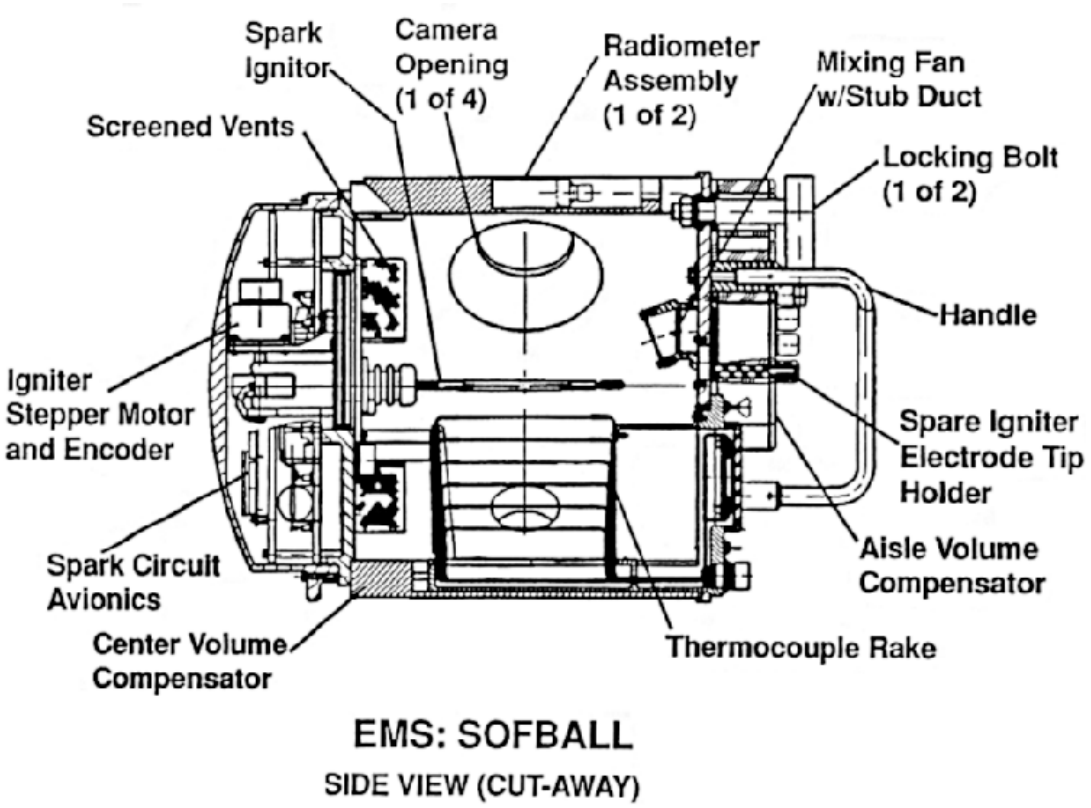

Figure 6. Schematic diagram of experimental apparatus test section.

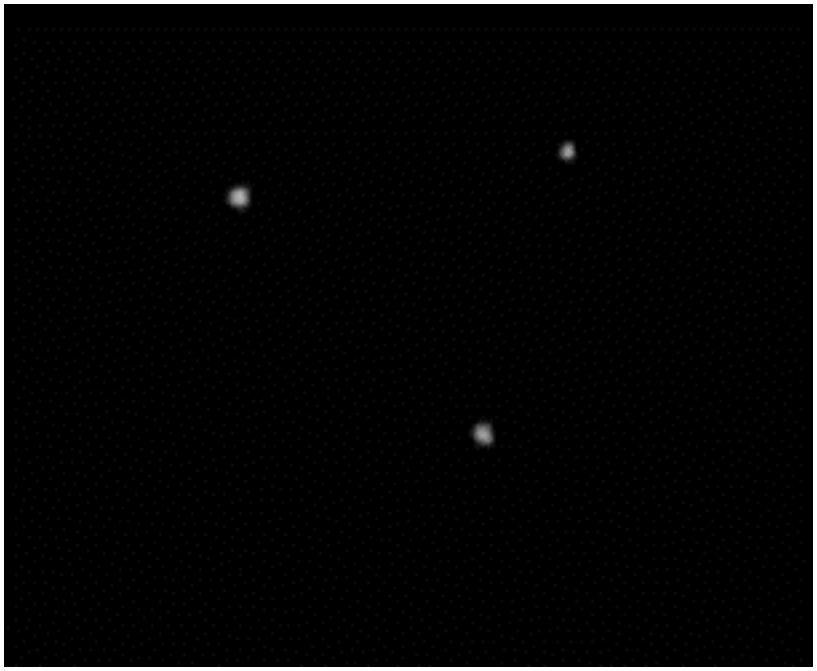

Figure 7. Image of flame obtained in 4.9% H_2 / 9.8% O_2 / 85.3% CO_2 mixture, taken 130 s after ignition. Field of view is 112 mm x 150 mm.

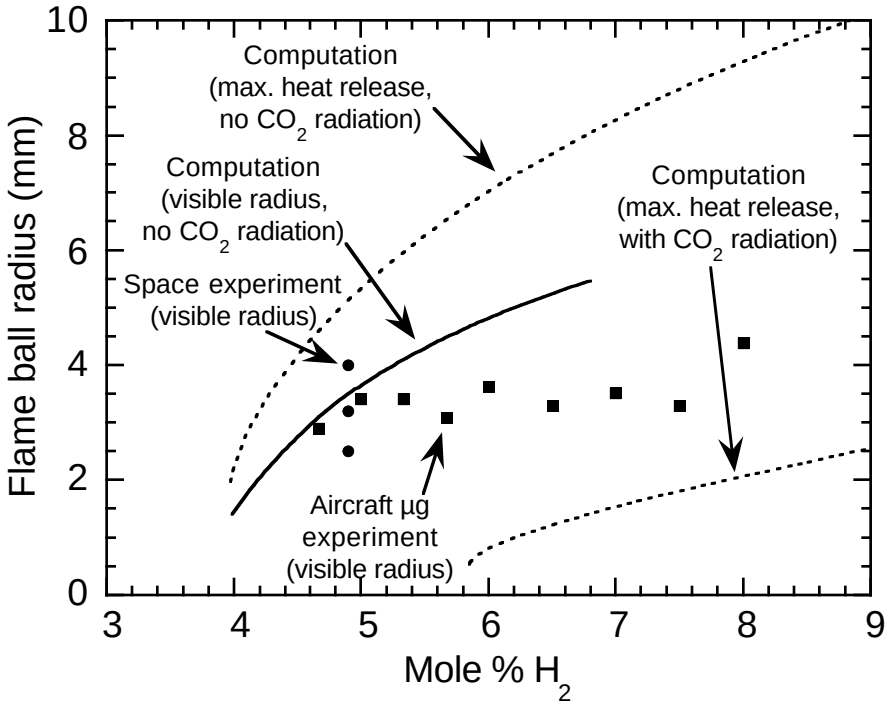

Figure 8. Predicted[13] visible flame ball radii in H_2-O_2-CO_2 mixtures (H_2:O_2 = 1:2) (solid curve) along with measured flame ball radii from aircraft µg experiments[7] (squares) and preliminary measured radii for SOFBALL Test #1 (circles). Also shown are predicted[13] flame ball radii based on radial location of maximum heat release including and excluding CO_2 radiation (dashed curves). The GRI chemical mechanism[17] is used in the predictions shown.

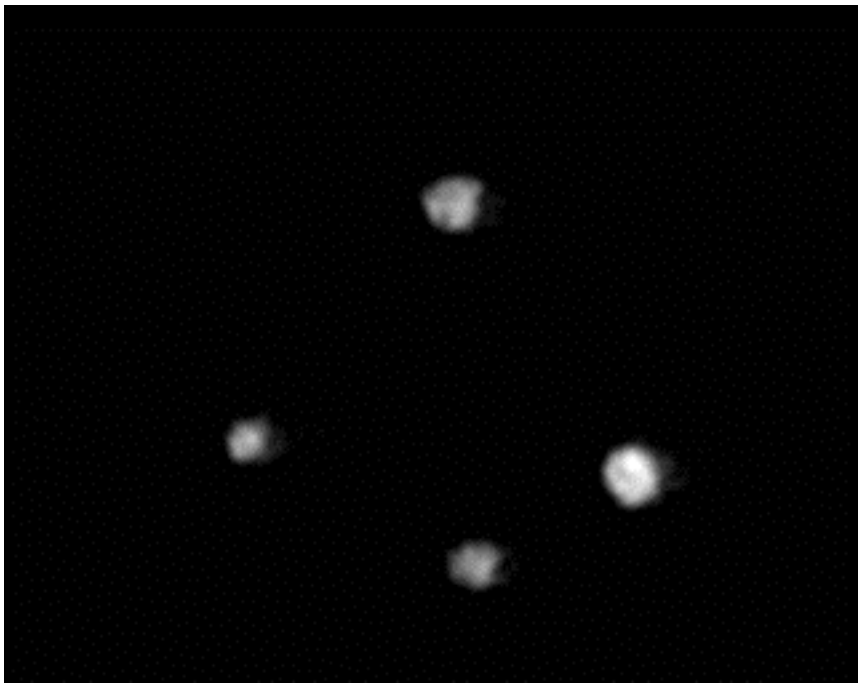

Figure 9. Image of flame balls obtained in 3.85% H_2 / 96.15% air mixture, taken 25 s after ignition. Field of view is 112 mm x 150 mm.

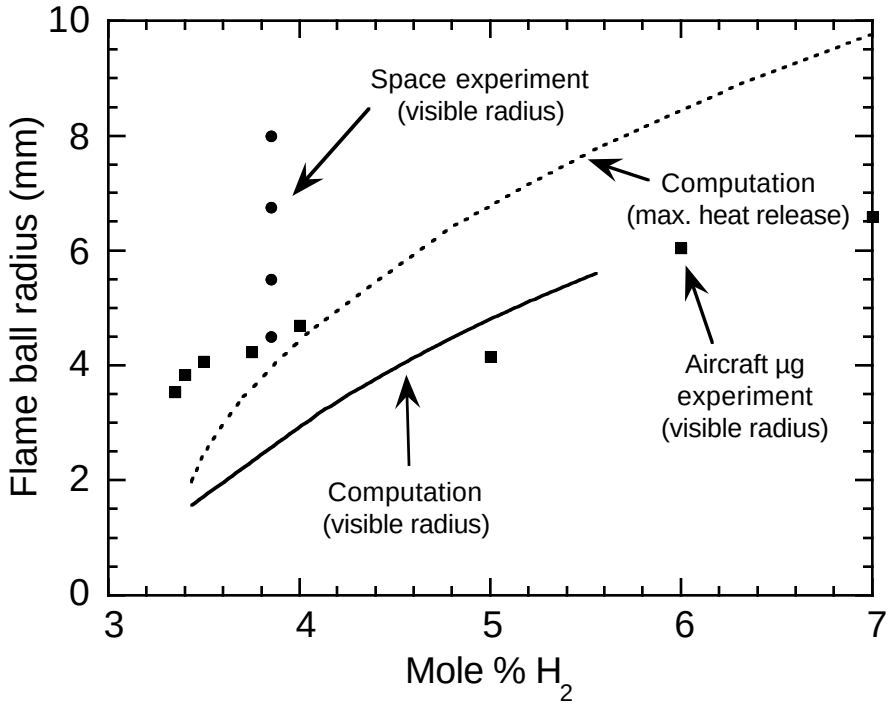

Figure 10. Predicted[13] visible flame ball radii in H_2-air mixtures (solid curve) along with measured flame ball radii from aircraft μg experiments[7] (squares) and preliminary measured radii for Test #2 (circles). Also shown are predicted[13] flame ball radii based on radial location of maximum heat release. The GRI chemical mechanism[17] is used in the predictions shown.

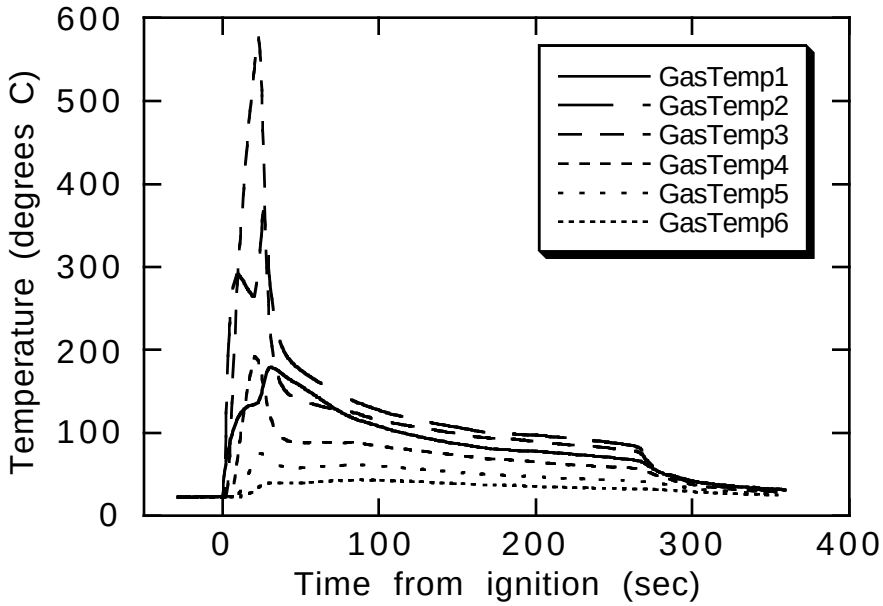

Figure 11. Measured gas temperatures for Test #2. Thermocouple locations corresponding to GasTemp1 through GasTemp6 are 30, 50, 70, 90, 110 and 130 mm from spark gap, respectively.

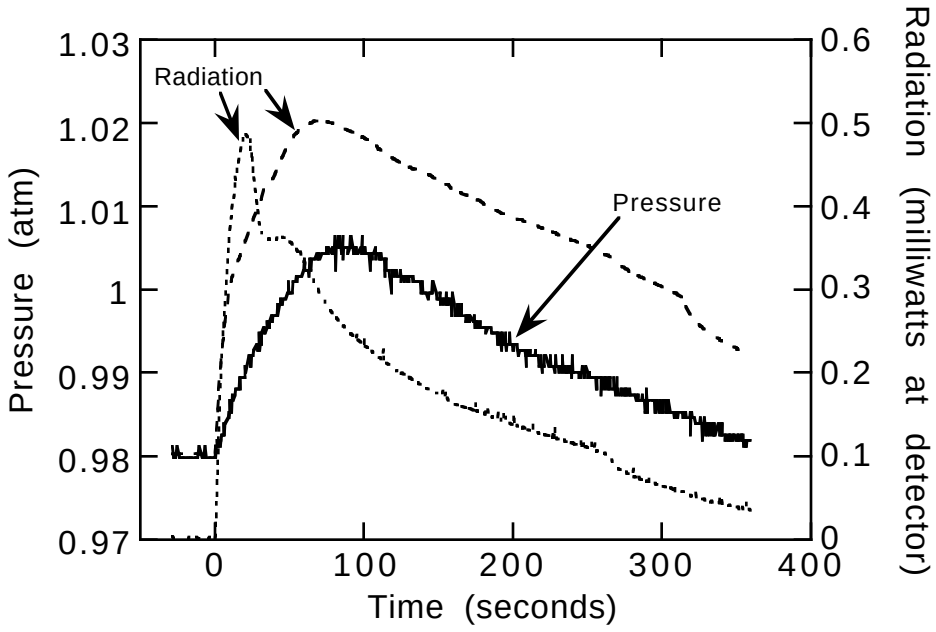

Figure 12. Measured chamber pressure and radiant emissions for Test #2.

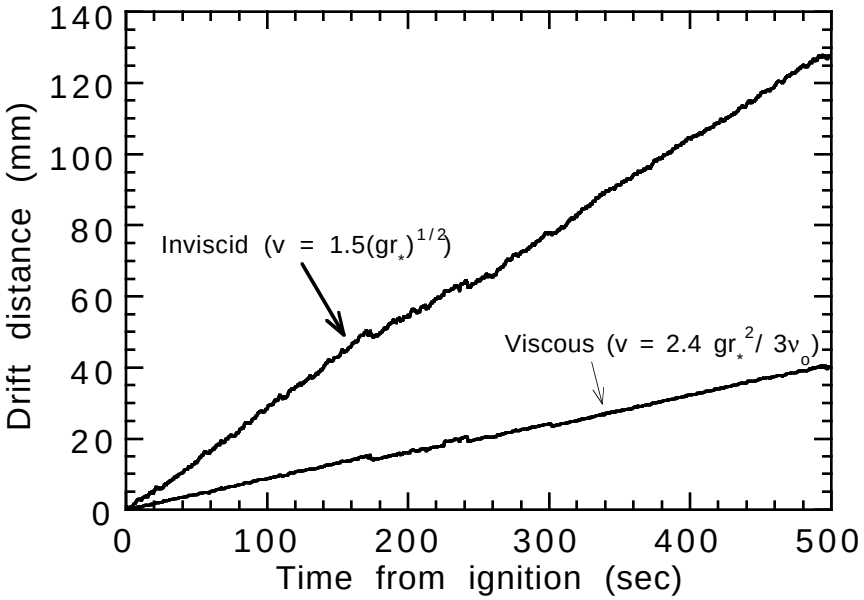

Figure 13. Flame ball drift distances predicted by the inviscid (Eq. (2)) and viscous (Eq. (4)) bubble rise relations for the conditions of Test #1, using acceleration data from the MMA/ASTRE system.

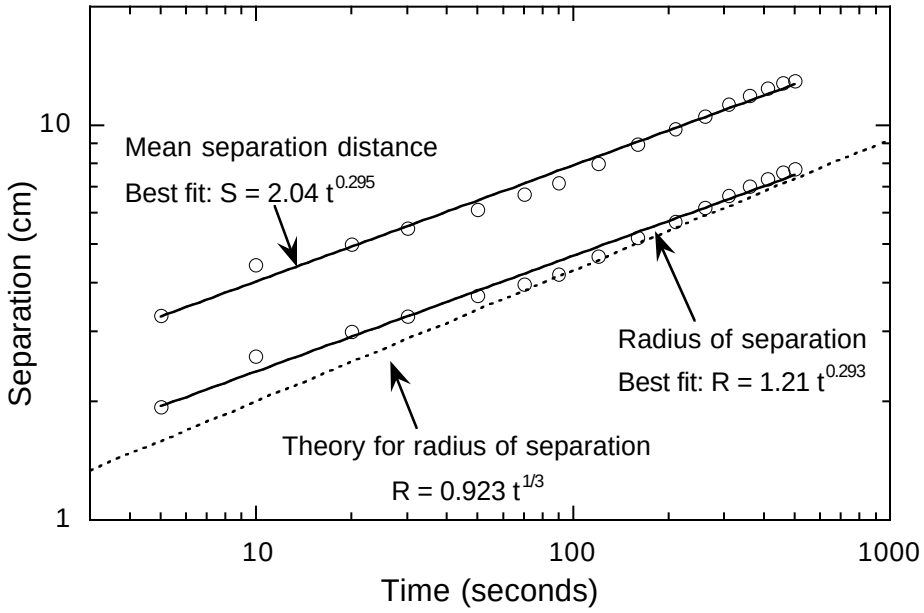

Figure 14. Observed radius of separation and mean separation of three flame balls in Test #1 as a function of time, and comparison to theoretical predictions[16].

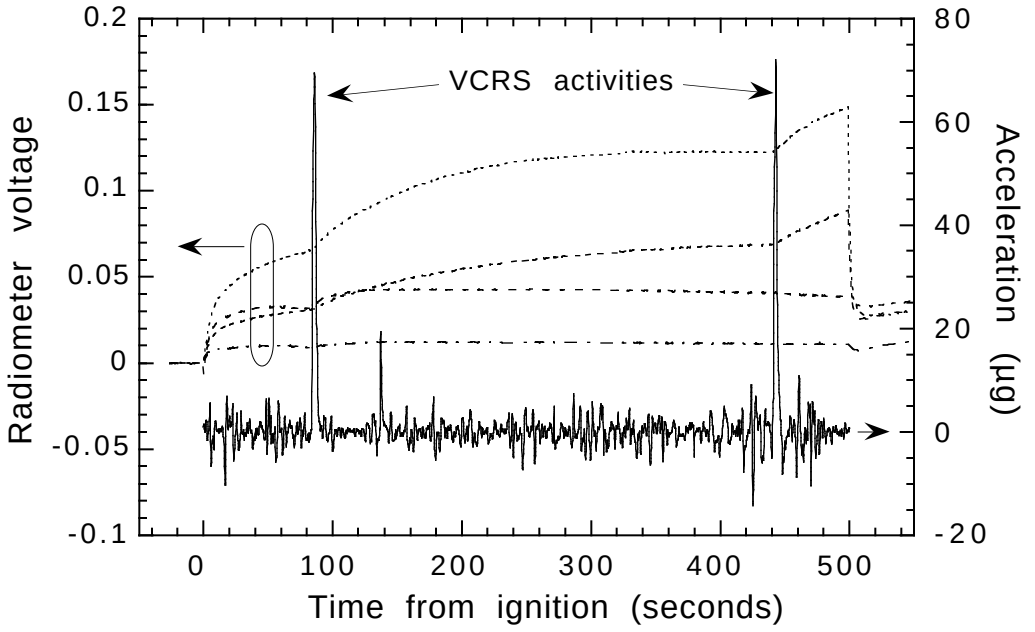

Figure 15. Example correlation of radiometer readings with Orbiter acceleration environment during STS-94 mission showing impact of Vernier Reaction Control System (VRCS) thruster firings. For clarity, only the Orbiter z-axis (vertical) acceleration component is shown. Mixture: 6.50% H_2 - 13.00% O_2 - 80.50% SF_6, 1 atm initial pressure. This test produced 1 flame ball.